Coherent topological defect dynamics and collective modes in superconductors and electronic crystals.

D. Mihailovic[1,2] **T.Mertelj**[1], **V.V.Kabanov**[1] **and S.Brazovskii**[3].

[1]Jozef Stefan Institute, Jamova 39, 1000 Ljubljana, Slovenia
[2]CENN Nanocenter, Jamova 39, 1000 Ljubljana, Slovenia
[3] LPTMS-CNRS, U. Paris-Sud, bat. 100, Cite Université, 91405 Orsay, France

Abstract. The control of condensed matter systems out of equilibrium by laser pulses allows us to investigate the system trajectories through symmetry-breaking phase transitions. Thus the evolution of both collective modes and single particle excitations can be followed through diverse phase transitions with femtosecond resolution. Here we present experimental observations of the order parameter trajectory in the normal→superconductor transition and charge-density wave ordering transitions. Of particular interest is the coherent evolution of topological defects forming during the transition via the Kibble-Zurek mechanism, which appears to be measurable in optical pump probe experiments. Experiments on CDW systems reveal some new phenomena, such as coherent oscillations of the order parameter, the creation and emission of dispersive amplitudon modes upon the annihilation of topological defects, and mixing with weakly coupled finite-frequency (massive) bosons.

1. Introduction.

The idea that non equilibrium phenomena in natural systems can be described in terms of a temporal evolution of a non-linear Landau expansion of the free energy has lead to theories as wide afield as elementary particles to cosmology. In condensed matter systems, where the idea originates, the opportunities for the study of the behaviour of nonlinear systems abound. However, typically, the study of these systems has been limited to near-equilibrium situations, where the system evolves slowly through the transition. Yet both particle physics experiments and cosmology distinctly deal with the temporal evolution of highly non-equilibrium systems. Typically one detects the decay products well after the decay itself, in the aftermath of the symmetry-breaking transition (SBT). Collisions of elementary particles, the subsequent creation of a high-symmetry intermediate state and its decay via symmetry-breaking interactions takes place on timescales which are well beyond the resolution of our current technology. Cosmological experiments being out of reach, experimental cosmological studies of the aftermath of the Big Bang reveal very complex behaviour in its aftermath, still beyond current theoretical understanding. As a result we have little insight into the non-equilibrium conditions close to the critical time t_c of the SBT when the creation of the new state is taking place.

In condensed matter systems the intrinsic dynamics of elementary excitations occur on timescales which are becoming accessible with current femtosecond laser technology. Particularly the normal-to-superconducting state transition and charge-density wave transition are of fundamental interest, as examples with different symmetry properties. Thus, typical single particle (quasiparticle) relaxation times in high-temperature superconductors are on timescales of 10^{-12} s [1], while electronic energy relaxation occurs on timescales of $10^{-12} - 10^{-13}$s [2]. Many body collective states have similar characteristic timescales. The so-called Ginzburg Landau (GL) time τ_{GL}, [3] which enters into the time-dependent GL equation is $\tau_{GL} \simeq 1/\Delta_s$ where Δ_s is the superconducting gap. For high-temperature superconductors, typical estimates give $\tau_{GL} \sim 10^{-13} - 10^{-12}$ s. In superconducting systems, the collective mode is overdamped, which means that it is difficult to discern the relaxation of the collective mode from single particle excitations. On the other hand, the characteristic timescale of collective mode in charge density wave systems is typically around $2\pi/\omega_{AM} \simeq 0.5 \times 10^{-12}$ s [4, 5]. Laser pulses can currently be created with sub femtosecond duration, so ample resolution is available for the study of the coherent evolution of collective modes in superconducting and charge-density-wave (CDW) systems. Moreover, by studying the concurrent evolution of the single particle spectrum, it may be possible to investigate the transient state of the underlying vacuum.

Following the suggestion by Zurek[6] of laboratory experiments to test Kibble's cosmological model [7], "system quench" experiments were performed in a number of different systems, including superconductors [8, 9], Bose-Einstein (BE) condensates within a trapped atomic gas [10] and polariton BE condensates [11]. Experiments on the Kibble-Zurek (KZ) mechanism so far have concentrated on the statistical analysis of topological defects left behind by the SBT, on timescales long compared to the intrinsic GL time τ_{GL}. Quench rates in these systems were relatively slow, the fastest being around 10^8K/s [9].

In standard optical Pump-probe *(P-p)* techniques (including THz probe) the response is related to the modulation of the dielectric constant (reflectivity or

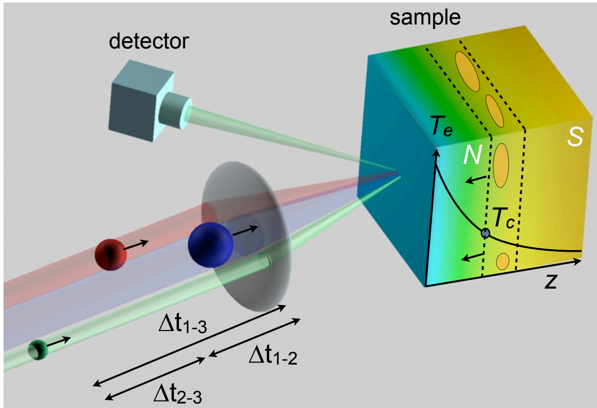

Figure 1. A schematic diagram of the three-pulse sequence and evolution of the superconducting order in a superconductor. The different time delays are indicated. The ratio of intensities of the D (blue ball), P(red ball) and p(green ball) laser pulses are typically 500:10:1 respectively. The electronic temperature decays into the sample as a result of the inhomogeneous excitation by laser light. The position of a normal/superconducting (N/S) state front, given by $T_e = T_c$ is rapidly moving towards the surface, leaving vortices in its wake. In a CDW system, the D pulse forces the system into the high-symmetry state, whereupon it undergoes a SBT as it cools. In the process, topological defects are created as a result of the inhomogeneity of the laser field.

absorbance), which can have a number of contributions in electronic systems such as superconductors and CDWs which are in one way or another related to the order parameter ψ: (1) the response due to hot carrier energy relaxation, (2) the quasiparticle (QP) recombination across the SC or CDW gap and (3) QP recombination across a pseudo-gap which is often present in these systems and (4) coherent phonon oscillations due to displacive excitation or impulsive Raman excitation. The coherent phonon oscillations cannot be distinguished from the oscillations of the order parameter with P-p spectroscopy. Moreover, different phonon modes are coupled to ψ to various degrees, and the dephasing is different for each mode, thus adding further to the complexity of the response from which it is difficult to extract the order parameter. We show that using a 3-pulse technique, these responses can be isolated to some extent, allowing us to study the coherent evolution of the order parameter with time though an SBT with very high temporal resolution. The method allows us to study the interactions of the collective mode of the CDW with other modes of different symmetry as well as annihilation of topological defects, revealing new finite frequency dispersive Higgs-like field excitations released as a result of domain wall annihilation.

2. Quench experiments with a multiple pulse all-optical technique.

The principle behind the technique involves the use of a multiple pulse trains to control the system and measure the time-response of the order parameter. A schematic diagram of the pulse sequence is shown in Fig. 1. A strong laser destruction (D) pulse - whose intensity is carefully adjusted to cause a perturbation of appropriate magnitude - is used to rapidly transfer the system from an ordered (broken symmetry)

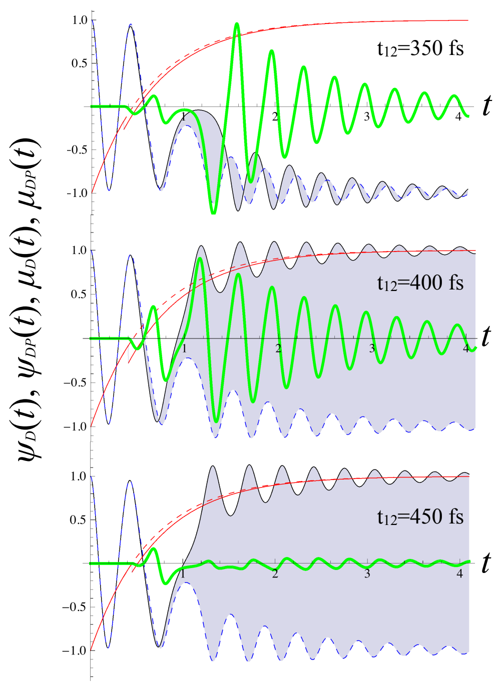

Figure 2. The calculated evolution of the order parameter $\psi_D(t)$ through the transition after an intense destruction D pulse at $t = 0$ (dashed blue line). When an additional P pulse is present, the trajectory $\psi_{DP}(t)$ (solid blue line) can be drastically modified, depending critically on Δt_{1-2}. The difference between the two is highlighted by the shaded areas. The evolution is calculated for three different time delays $\Delta t_{1-2} = 350, 400$ and 450 fs. The intensity of the P pulse is 10% of the intensity of the D pulse. The calculation in this figure is done with an exponential perturbation function $\mu(t)$ for the D pulse (shown by the dashed red line) and $\mu_{DP}(t)$ with both pulses (solid red line). The green line is the response function in reflectivity predicted according to Eq. 10.

state to the disordered (high-symmetry) state, whereafter the system reverts back to equilibrium through the SBT. The state of the system at any given time after the D pulse is determined by standard pump-probe spectroscopy sequence, which involves first exciting the system by an additional weak perturbing P pulse delayed by Δt_{1-2} with respect to the D pulse, and subsequently measuring the resulting change of reflectivity $\Delta R/R$ of the sample by a weak probe (p) pulse (see Fig. 1). In sec. 3.1 we will show how the optical response $\Delta R/R$ can be related to the order parameter in superconductors and CDW systems.

On the level of field theory, the trajectory of the system through the SBT can be modeled within time-dependent Ginzburg Landau theory with a free energy functional corresponding to the symmetry of the problem in hand. For a charge density wave system, to capture the salient physics, we can assume an order parameter $\Psi = A(t, \mathbf{r})e^{i\phi}$ and make the assumption that the relaxation on phase ϕ is slow compared to τ_{GL}, which means that the trajectory is dominated by the dynamics of

A(t,r) [12, 13]:

$$\frac{\partial^2 A}{\partial t^2}+\Gamma\omega_{AM}\frac{\partial A}{\partial t}-\alpha(t,\mathrm{r})\omega_{AM}^2 A+\omega_{AM}^2 A^3-\xi^2\omega_{AM}^2\frac{\partial^2 A}{\partial z^2}=0, \quad (1)$$

where ω_{AM} is the angular frequency of the collective amplitude mode, ξ is the coherence length, $\Gamma = \Delta\omega_{AM}/\omega_{AM}$ is the damping of the AM, and $\alpha(t,\mathbf{r})$ is temporally and spatially dependent and is derived from the usual GL temperature $\alpha(t,\mathbf{r}) = 1-\mu(t,\mathbf{r})$ describes the control parameter. $\mu(t,\mathbf{r})$ may be $T(t,\mathbf{r})/T_c$, as given by original GL theory, or may be approximated by an exponential function which signifies the cooling of the system. The spatial variation of the light intensity is accounted for by an excitation function $\mu(t,z)=\frac{T_e(t,z)}{T_c}\exp(-z/\lambda)$ where λ is the optical penetration depth. Using experimental values for $\nu_{AM}=\omega_{AM}/2\pi = 2.4$ THz, the line-width $\Delta\nu_{AM} = 0.05$ THz and coherence length $\xi = 1$ nm [12] we can compute $A(t,z)$.

In 3-pulse experiments, the P pulse presents an additional perturbation which can modify the trajectory, especially if it occurs close to the critical time t_c. In Fig. 2 we show calculated trajectories of ψ for three different delay times Δt_{1-2} of the P pulse with respect to the D pulse. The "butterfly effect" is very evident: ψ may end up as either $+1$ or -1, critically depending on Δt_{1-2}.

The equation of motion for a superconductor within the time-dependent Ginzburg-Landau (TDGL) model is more complicated because the excitations are charged and ψ is coupled to the electro-magnetic field, and are usually considered to be overdamped, so they do not include any second-order time-derivative:

$$u\left(\frac{\partial\psi}{\partial t}+i\Phi\psi\right)=-\alpha_r(t,\mathbf{r})\psi-\psi|\psi|^2-(i\nabla+\mathbf{a})^2\psi+\eta \quad (2)$$

$$\nabla^2\Phi=-\nabla\Big[\frac{i}{2}(\psi^*\nabla\psi-\psi\nabla\psi^*)+\mathbf{a}|\psi|^2\Big]. \quad (3)$$

These equations have been used for analytic and numeric analyses of dynamics of topological defects (vortices and phase slips) in superconducting wires, as reviewed in [14, 15]. The vector potential $\mathbf{a}$ is written in units of $\frac{\phi_0}{2\pi\xi}$ (ϕ_0 is the flux quantum, ξ is the coherence length) and the electrostatic potential Φ in units of $\frac{\hbar}{2e\tau_\theta}$, with e being the elementary charge, τ_θ is the transverse relaxation time and $\hbar$ the reduced Planck constant. The only dimensionless parameter left in the equation is the ratio $u=\frac{\tau_\rho}{\tau_\theta}$ between the longitudinal relaxation time and the transverse relaxation time. Typically, for high-temperature superconductors $\tau_\theta \approx 1$ ps and $u \approx 5$ [15]. The Langevin noise term η introduces microscopic fluctuations into the dynamics [15].

3. Control of the quench rate and optical response function

In the simplest approximation, suggested by the usual α parameter in the GL equations, the excitation function μ can be the system temperature. In the case where the electronic system is being discussed, such as superconductors and CDWs, it is the electronic temperature $T_e(t)$ which is the relevant control parameter. In recent years, significant progress has been made in understanding the time evolution of electron and lattice temperatures in superconductors and CDWs following excitation by a laser pulse. The quench rate is determined by the energy relaxation rate of electrons at early times up to ∼1 ps, and the lattice $T_L(t)$ on longer timescales (tens of picoseconds and beyond). The time-evolution of $T_e(t)$ and $T_{\mathrm{L}}(t)$ respectively, which

govern the quench process, may be estimated using a two-temperature model [16]: $\gamma_{\mathrm{e}} T_{\mathrm{e}} \frac{dT_{\mathrm{e}}}{dt} = -\gamma_{\mathrm{L}}(T_{\mathrm{e}} - T_{\mathrm{L}}) + E(t)$ and $C_{\mathrm{L}}(T)\frac{dT_{\mathrm{L}}}{dt} = \gamma_{\mathrm{L}}(T_{\mathrm{e}} - T_{\mathrm{L}})$, where $E(t)$ is a function (Gaussian) describing the energy density per unit time supplied by the laser pulse. The pulse energy $E_D = E_p/d^2$ where E_p is the pulse energy. We used the temperature-dependent thermal constants $\gamma_{\mathrm{e}}(T)$ and $C_{\mathrm{L}}(T)$ from experimental data[19] and the measured energy loss rate $\gamma_{\mathrm{L}} \simeq 340$ K/ps for $La_{1.9}Sr_{0.1}CuO_4$ [2]. The dependence of $T_{\mathrm{e}}(t)$ and $T_{\mathrm{L}}(t)$ on the energy density per pulse $U = \int E(t)dt$ is shown in Fig. 3a) for the first few picoseconds. The red contour lines show when either T_{e} or T_{L} crosses T_{c}. Initially, the rate of cooling $\gamma_e = \frac{dT_e}{dt}$ is very rapid until T_e reaches T_L. Thereafter, T_e follows T_L, and is dominated by phonon anharmonic decay or phonon escape and thermal diffusion processes, all of which are much slower than electronic energy loss. Thus, to change the quench rate we can adjust the energy density U_D of the D pulses, so that the system either cools rapidly through electron thermalization, or more slowly by phonon decay and diffusion processes. As shown in Fig. 3a), for low U_D, only T_e exceeds T_c, so the quench back through T_c will be fast and dominated by electronic cooling. For larger U_D, T_L exceeds T_c, so on cooling the quench rate though T_c is significantly slower and dominated by lattice cooling.

3.1. The response function

The key issue is detection of the order parameter through the SBT. Here we show how for superconductors and CDW systems, the response measured in 3-pulse experiments is related to the order parameter. While a full kinetic theory which would take into account single particle and phonon relaxation processes through the transition is beyond reach at present, we can obtain good approximations for the quasiparticle response functions in superconductors and collective mode in CDW systems respectively based on well-accepted phenomenological theory.

The temperature dependence of the difference of the optical reflectivity between the superconducting state R_s and the normal state R_n in a superconductor has been found to be described very well by an expression derived from the Mattis-Bardeen formula [20]:

$$R_s(T) - R_n = A\frac{\Delta(T)^2}{\omega^2} ln\left[\frac{1.47\omega}{\Delta(T)}\right] \tag{4}$$

where $\Delta(T) = 1 - (T/T_c)^2$ is usually used to describe the temperature dependence of the gap, ω is the frequency of light in units of $\hbar$, R_n is the reflectivity in the normal state. We need to calculate the transient change of reflectivity δR, as the system is evolving through the transition in time, so we explicitly replace $\Delta(T)$ with $\Delta(t)$. Using the 2-fluid model, we substitute $\Delta^2 = \Delta_0^2 n_s = \Delta_0^2(1 - n_q)$, where n_s is the superfluid density and n_q is the quasiparticle density, and Δ_0 is the gap at $T = 0$. We can relate δR to the photo-excited carrier density n_p using the fact that $\delta n_q = n_p$:

$$\delta R = \frac{\partial R}{\partial \Delta}\frac{\partial \Delta}{\partial n_q}\delta n_q = \frac{A\Delta_0^2}{2\omega^2}\left(1 - 2ln\left[\frac{1.47\omega}{\Delta(t)}\right]\right) n_p \tag{5}$$

If we ignore the derivative of the logarithmic correction with respect to Δ, substituting Δ_0 for $\Delta(t)$ in the logarithm, we obtain $R_s(t) - R_n \simeq A\frac{\Delta(t)^2}{\omega^2} ln\left[\frac{1.47\omega}{\Delta_0}\right]$. δR then simplifies to:

$$\delta R = \frac{\partial R}{\partial \Delta}\frac{\partial \Delta}{\partial n_q}\delta n_q = \frac{2A\Delta(t)}{\omega^2}\delta\Delta \propto -\frac{A\Delta_0^2}{\omega^2} n_p. \tag{6}$$

Under near-bottleneck conditions, when the QPs and the phonons are in near-equilibrium, n_p is given by [21]:

$$n_p = \frac{1/(\Delta(T(t))) + T(t)/2)}{1 + B\sqrt{2T(t)/(\Delta(T(t))}\mathrm{Exp}[-\Delta(T(t))/T(t)]}. \tag{7}$$

where Δ is the superconducting gap, $B = \nu/N(0)\hbar\Omega_c$, where ν is the effective number of phonon modes of frequency $\hbar\Omega_c$ per unit cell participating in the relaxation process. Here we have explicitly written the temperature T to be time dependent. B can be determined by fitting the temperature dependence of $\Delta R/R$ and $N(0)$ is the density of electronic states at the Fermi energy. Substituting $\Delta_0\psi(t)$ for $\Delta(t)$ from the solution of Eq. 3, we obtain:

$$\delta R/R \propto \frac{A\Delta_0^2}{2\omega^2}\left(1 - 2ln\left[\frac{1.47\omega}{\Delta\,(t)}\right]\right)\frac{1/(\Delta_0|\psi(t)| + T(t)/2)}{1 + B\sqrt{2T(t)/\Delta_0|\psi(t)|}\mathrm{Exp}[-\Delta_0|\psi(t)|/T(t)]} \tag{8}$$

The response functions using the appropriate constants for $La_{1.9}Sr_{0.1}CuO_4$ are plotted in Fig. 3, together with the time evolution of $T_e(t)$ for $E = 1.6$ J/cm^3, and the order parameter $|\psi(t)|$ and $|\psi(t)|^2$ for the case of a homogeneous superconductor calculated using Eq. 2 in the absence of fieled $\mathbf{a} = \mathbf{0}$, and $\Phi = 0$. The experimental reflectivity response $\delta R/R$ is close to the square of the order parameter $|\psi|^2$ over a large range of t, particularly for large ψ. The calculated case for an inhomogeneous superconductor which takes into account the depth profile of the laser beam is discussed in the next section where it is compared with experimental data.

In CDWs, when discussing the transient response of collective amplitude mode, the response is related to the displacement ΔR of the atoms from equilibrium position R_0, where $\Delta R \propto \psi - \psi_0$, where ψ_0 is the equilibrium value of the order parameter. To obtain the optical response, we can expand the dielectric constant near CDW phase transition in powers of the order parameter [17]:

$$\epsilon = \epsilon_0 + c_2|\psi|^2. \tag{9}$$

Here ϵ_0 is the dielectric constant of the high temperature symmetric phase, c_2 is a real constant.

The relevant response in *D-P-p* experiments can be expressed in terms of the difference between the response *with* and *without* the P pulse, proportional to $\Delta|\psi|^2$, so to first order [12]:

$$\frac{\Delta R}{R} \simeq \frac{\Delta\epsilon}{\epsilon} \propto \psi_{DP}^2(t, \mathbf{r}, \Delta t_{12}) - \psi_D^2(t, \mathbf{r}). \tag{10}$$

This response has been tested for the case of the CDW transition in $TbTe_3$ [12]. We see that by careful design of the experimental probe and the use of 3 pulse techniques, it is possible to identify and even isolate the dominant contribution to the optical response which is related to the order parameter, thus providing valuable information of the temporal evolution of ψ by measurement of either single particle and collective excitations through the SBT.

4. Superconductors: probing vortex dynamics on the picosecond timescale.

In Figure 4a) we show the time-evolution of $\delta R/R$ in $La_{1.9}Sr_{0.1}CuO_4$ measured with a $P - p$ sequence at a sample base temperature of 4 K after a 50 fs laser pulse. All

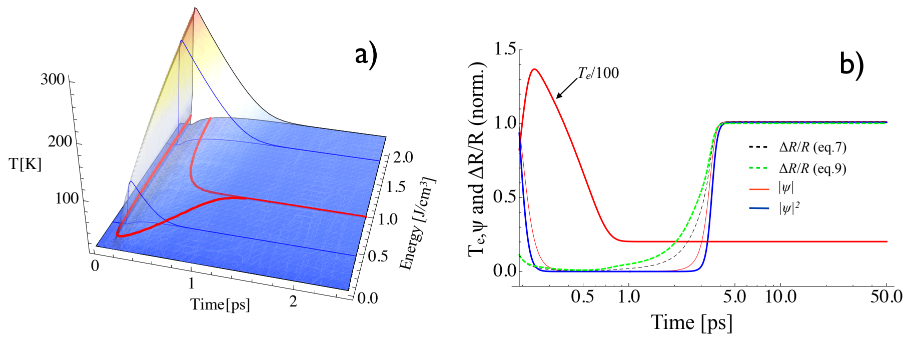

Figure 3. a) The calculated evolution of T_e, T_L as a function of D pulse energy. b) The order parameter $|\psi|$ and reflectivity response $\Delta R/R$ as a function of time through the quench. The calculation of T_e and T_L is performed using the two-temperature model [18, 16] using the appropriate specific heat and thermal conductivity functions for $La_{1.9}Sr_{0.1}CuO_4$ from experimental data [20]. The response functions compare the response calculated with Eq. 8 and 6 with $|\psi|$ and $|\psi|^2$.

laser pulses have a wavelength of 800 nm. The D pulse energy $E_{\mathrm{D}} = 0.8$ J/cm^3 is adjusted to heat the sample above T_c. (The threshold values for the destruction of the SC state were previously reported in [20]).

According to Eq. 7, the QP amplitude in *P*-*p* experiments are related to $|\psi|$, which allows us to compare the data with the calculated trajectory based on a solution of Eqs. 2 and 3. The numerical solution calculated without the fluctuation term η is shown by the solid line in Fig. 4a). Comparing with the measured data, we see that the prediction is remarkably good overall, except for a depression of the order parameter of approximately 10-20 % between 10 and 30 ps. This discrepancy may be attributed to vortices which form as a result of the fast quench through T_c. $\psi \to 0$ in the vortex cores, so the spatially averaged value of ψ will be depressed if they are present. To try and model the effect of vortices we compare calculations with and without the fluctuation term η, while keeping all other parameters unchanged. The introduction of fluctuations gives rise to a depression of $|\psi|$ in the region around 10 ps, shown by the dashed line in Fig. 4b). Qualitatively, we see that the presence of vortices may explain the depression of the order parameter around 10 ps in $La_{1.9}Sr_{0.1}CuO_4$. Considering the simplicity of both the TDGL model and the crudeness of the approximations for the response function (Eq. 7), the agreement between data and theory is quite reasonable.

5. Topological defects in CDWs: coherent dynamics.

Transition metal tri-tellurides such as $DyTe_3$ are excellent systems for femtosecond measurements of system trajectories through SBTs to a CDW state. Recently, the evolution of single particle and collective excitations though the CDW transition have been reported in $TbTe_3$ [12]. Here we show the temporal evolution of the order parameter in a related material, $DyTe_3$, which undergoes a transition to a CDW state at 305K. The temporal evolution of the collective mode spectrum after the D pulse is shown in Fig. 5. The spectrum was obtained from the Fourier transform of the

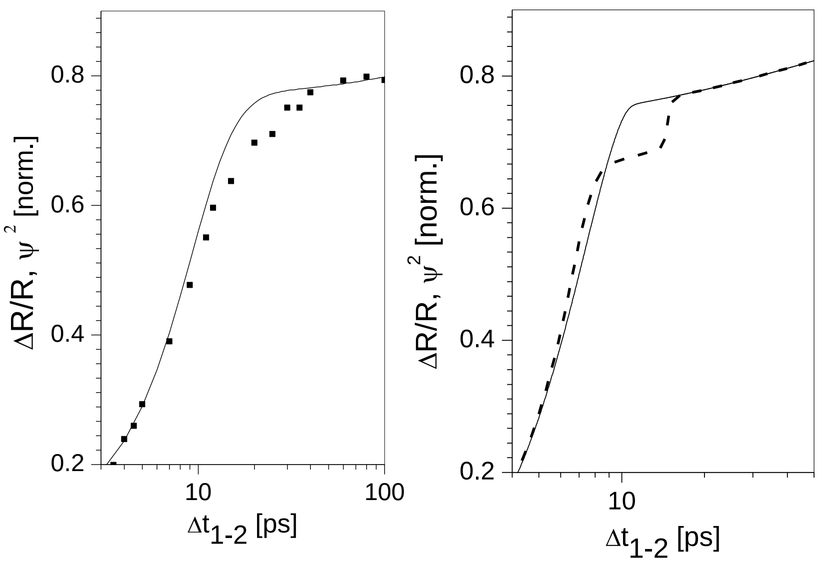

Figure 4. The recovery of the order parameter ψ after an ultrafast quench in $La_{1.9}Sr_{0.1}CuO_4$. The data points (left panel) represent the dependence of the maximum $\Delta R/R$ response as a function of Δt_{1-2}, while the solid curve is the trajectory of $|\psi(t)|^2$ calculated from Eq. 3, normalized to the value at long times after the D pulse. The right panel shows the calculated trajectory when fluctuations are included in Eq. 3 via the η term (dashed line). The trajectory without noise η is included for reference (black line) for the same parameters. The difference between the two is attributed to the effect of vortices spontaneously created via the KZ mechanism, which annihilate on a timescale of 20 ps according to theory predictions. A comparison with the data suggests the formation of vortices in $La_{1.9}Sr_{0.1}CuO_4$ created in the quench on a timescale between 10 and 30 ps. Note that we have limited ourselves to the time interval where $\psi \to \psi_{equilibrium}$, so $\Delta R/R \propto |\psi|$ is a valid approximation (see Fig. 3b)).

transient reflectivity ΔR/R recorded at each Δt_{1-2} as a function of Δt_{2-3}. We identify two modes in the spectra at ∼1.68 THz and ∼ 2.2 THz at long times $\Delta t_{1-2} > 10$ ps. The latter is assigned to the amplitude mode (AM) of the CDW based on its distinct temperature dependence [5], while the former is a phonon mode (PM). At $t \simeq 1.3$ ps, the AM exhibits mixing with the PM. Oscillations of the order parameter are clearly visible at short times and appear as modulations of the intensity of both modes occurring up to ∼ 8 ps. At longer times, the intensity oscillations and the frequency recovers to 2.2 THz after 4×10^6 ps. No further relaxation takes place beyond this timescale.

In Fig. 6 a) we show the calculated $\psi(z,t)$ from Eq. 1 using parameters for $DyTe_3$: $\omega_{AM} = 2.2$ THz, the AM linewidth $\Gamma = 0.3$ THz, and coherence length $\xi = 1.3$ nm from [24]. For simplicity, the driving term $\alpha(t,z)$ in Eq. 1 is assumed to be exponential

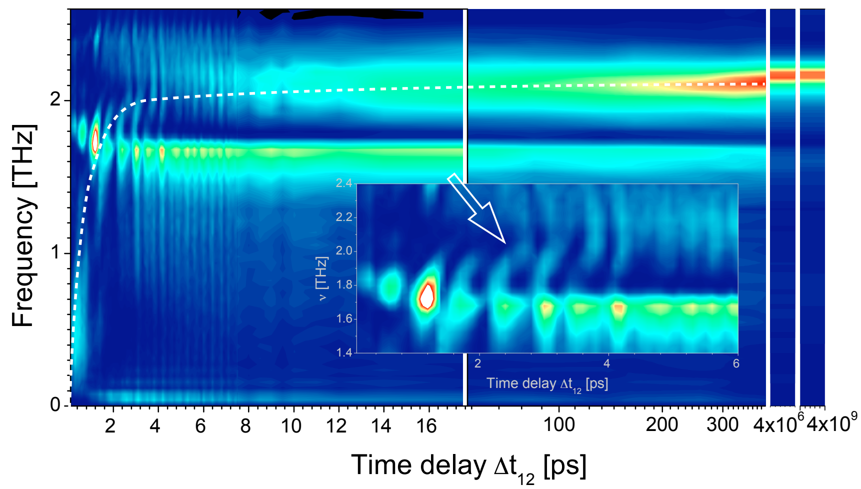

Figure 5. The temporal evolution of the collective mode spectrum in $DyTe_3$ through the quench into the ordered phase. The plot shows the amplitude of the spectrum obtained from the transient reflectivity $\Delta R/R$ as a function of Δt_{2-3} for different Δt_{1-2}. The AM shows some intensity around 0.5 THz at short times, then crosses a phonon at 1.68 THz at around 2 ps and eventually settles down to 2.2 THz at long times. The dotted line shows the recovery of the electronic single particle gap determined from the recovery of the SP peak scaled onto the $\omega - \Delta t_{1-2}$ plot. At early times, coherent oscillations of the order parameter cause fluctuations of the intensity of the AM and the 1.68 THz phonon. Interference between the phonon and the AM is clearly observed, including a renormalization of the phonon frequency from $\sim$ 1.85 THz at early times (in the high-symmetry state) to 1.68 THz in the ordered state. The insert shows the dynamics at short times. Distortions of the line-shapes in time are attributed to the presence of topological defects created in the quench to the CDW state (see arrow) on the basis of comparisons between theory and experiment (see Fig. 6). The sample base temperature is 4 K throughout the experiment. The color scale is normalized, so that the maximum amplitude is 1 (red). (In the insert, the scale is expanded to show the additional spectral features shown by the arrow.)

in time and in space: $\alpha = exp(-t/\tau - z/\lambda)$, where the penetration depth is given by the experimental value $\lambda = 20$ nm [25]. The calculation predicts the formation of three domains created within the first picosecond, parallel to the surface, with domain walls at $\sim$ 30 nm and $\sim$ 45 nm. After 5 ps, the domains walls are annihilated, leaving behind a single domain. The event is accompanied by the emission of a finite frequency dispersive amplitude waves traveling towards the surface and into the sample. The velocity of the amplitude wave is seen from Fig. 6 to be approximately $v_A \simeq 10$ nm/ps. The wave reaches the surface with 6-8 ps causing a disturbance of the AM which is visible as a temporal distortion of the AM spectral line-shape. (The insert to Fig. 5 highlights the distortions of $\omega - \Delta t_{12}$ spectra). The calculated spectrum

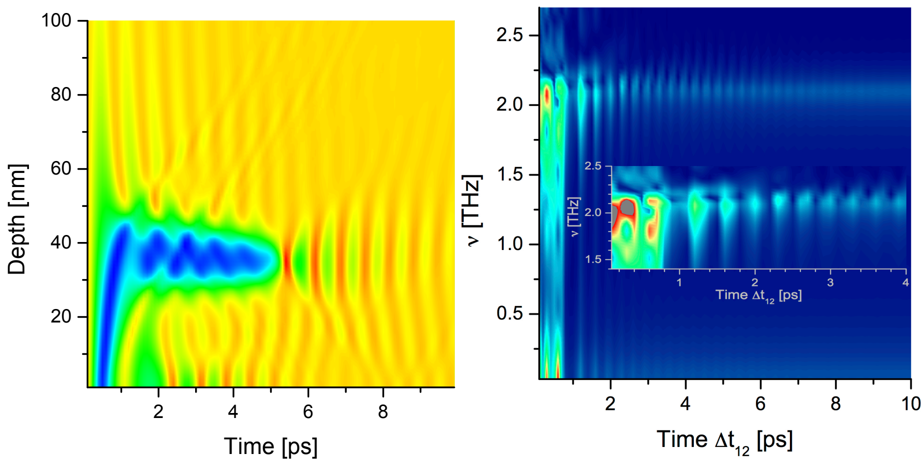

Figure 6. a) The calculated order parameter (colour scale) as a function of time and depth into the sample after a laser pulse as a solution to Eq. 1 and parameters for $DyTe_3$. b) The intensity oscillations are calculated from Eq. 10, taking into account the appropriate boundary conditions and inhomogeneity of the laser field in Eq. 1. Distortions to the line-shapes are attributed to the annihilation of topological defects, similarly as observed in $TbTe_3$ [12]. The color scale is normalized, so that the maximum amplitude is 1 (red) and minimum is -1 (blue). (In the insert, the color scale is expanded to show the additional spectral features)

(using Eq. 10) is shown in Fig. b). The predicted distortions have a great deal of similarity with the experimentally observed evolution of the spectrum shown in Fig. 5. Unfortunately the presence of the phonon interference in this material complicates the detailed comparison between theory and experiment. Similar, although more pronounced distortions were observed in $TbTe_3$, where the interference from other phonons is less problematic [12].

In [26] it is further shown that incoherent intrinsic topological defect dynamics in the related system $TbTe_3$ occurs on a timescale of ~ 30 ps, similar to the timescale of vortex annihilation dynamics inferred from the experiments on $La_{1.9}Sr_{0.1}CuO_4$. The experiments show that pinned-defect-related annihilation appears to be present on much longer timescales of $10^{-10} - 10^{-6}$ s.

6. Discussion

We have demonstrated that femtosecond optical experiments with multiple pulse techniques open the way to detailed studies of the temporal dynamics of systems undergoing SBTs and can be interpreted in the context of a phenomenological field theory without resort to microscopic theory. The basic analogy with cosmology and elementary particle collisions comes from the fact that the SBT take place in temporally evolving systems with high temperature intial conditions. Single particle fermionic and collective bosonic excitations can be unambiguously identified and related to the temporal evolution of the order parameter through the transition and topological defects (domain walls and vortices) are shown to lead to experimentally observable phenomena. It appears that CDWs are eminently more suitable for investigation of topological defects than superconductors because the collective mode

conveys significantly more information of the system trajectory than single-particle excitations, particularly relating to coherent defect dynamics. We have shown that by adjusting the laser excitation energy density, the quench rate can be varied and controlled, leading to the possibility of investigating domain wall recombination. Further studies as a function of quench rate and temperature may be expected to reveal systematic behaviour, which can be related to the predictions of the KZ mechanism for the generation of topological defects. In the context of the discussion regarding the possible cosmological importance of creation and annihilation of cosmic domains and strings [7], the present paper demonstrates that *coherent* creation and annihilation of topological defects leads to observable consequences in condensed matter systems. Contrary to previous experiments, the distinction between coherent and incoherent recombination dynamics, as well as intrinsic and extrinsic defect-related annihilation is quite clear, because the rates of decay are vastly different: coherent domain recombination occurs on a $\tau_{coh} \simeq 3$ ps timescale, while intrinsic incoherent domain wall recombination timescale is $\tau_i \simeq 30$ ps. Finally, extrinsic defect-related dynamics occurs on timescales of $\tau_{ext} \sim 100$ ps or longer [26]. The experiments thus establish a hierarchy of timescales associated with the annihilation of topological defects.

The evolution of the single particle response as a function of time after destruction by a laser pulse in the $La_{1.9}Sr_{0.1}CuO_4$ superconductor suggests that a depression of the order parameter compared with the theory prediction can be understood if vortices are included in the within an inhomogeneous model, suggesting intrinsic vortex creation and annihilation in $La_{1.9}Sr_{0.1}CuO_4$ takes place on a timescale of 10-20 ps. Although one might argue that the discrepancy between the trajectory of $|\psi|$ and the measured response may be attributed to breakdown of the approximations made in deriving the response function Eq. 7, these problems are not expected to be important in the region around 10-20 ps, but rather at shorter times, closer to t_c: when $\psi \to 1$, the gap is fully developed, and the QP response is expected to be described well by the Rothwarf-Taylor model in the bottleneck regime[23], where the gap $\Delta(t) \to 1$ and is almost constant, so Eq. 7 is reasonably valid, as shown in Fig. 3.

We point out that in the context of more general field theories of related time-evolving systems, apart from the AM, two other bosons observed in CDW systems are of interest. The first is created as a result of the annihilation of domain walls shown in Fig. 6. Upon annihilation, two finite-frequency (massive) $\psi-$waves are emitted which propagate perpendicular to the surface into the sample and towards the surface. Calculations of the "wave effect" on the temporal evolution of the AM spectral shape appear to be confirmed by experiments in $DyTe_3$ (discussed here) and in $TbTe_3$ [12].

The second bosonic excitation of interest is the phonon mode (PM) with an equilibrium frequency of ω_{PM} =1.68 THz. The time-evolution of this mode is very different from the evolution of the AM: it does not show critical behaviour near t_c. Instead its frequency is just slightly renormalized in the low symmetry state. Before t_c, the PM frequency is ω_{PM} $=1.85 \pm 0.02$ THz. Because its frequency ω_{PM} in the ordered state is lower than ω_{AM} $(= 2.2$ THz), it crosses the AM as the latter hardens after t_c as indicated in Fig. 5. At $\Delta t_{12} \simeq 1.3$ ps the AM interferes with the PM, and the phonon frequency is renormalized for $\Delta t_{12} > 2$ ps, to $\omega_{AM} = 1.68 \pm 0.02$ THz.

In experiments where the control parameter is temperature T rather than time, this behaviour is well understood [5]: below the critical temperature T_c, as the AM hardens with decreasing T, it crosses the PM at some intermediate temperature, displaying mode mixing. The coupling of the AM and the PM in compounds such as

$DyTe_3$ is relatively weak, the off-diagonal matrix element being $\delta \simeq 0.1 \pm 0.01$ THz [5]. The PMs form a large reservoir of excitations which are weakly coupled to the order parameter. The symmetry of the PM plays an important role in the temporal behaviour. By definition, the order parameter is totally symmetric, (A representation) so even-symmetry modes are expected to couple strongly to it. When the system has inversion symmetry, such as here, ($DyTe_3$ has D_{2h} point group symmetry) the odd-symmetry modes do not couple to the ψ to first order. Odd symmetry modes thus display some characteristics of weakly interacting massive particles in cosmology. The observed PM has a large mass (frequency) and is weakly coupled to the order parameter, either because they have inappropriate symmetry (in which case the weak coupling comes from higher order interactions), or the matrix element coupling to A symmetry excitations is small. In contrast to the AM and the fermionic excitations which emerge after the SBT takes place, the PM excitations exist *before* the SBT (i.e. before and after the Big Bang within the cosmological paradigm). By analogy with the PM, dark matter excitations may be thought of as a remnant excitations from before t_c. As such they are external to the GL (or Standard) model.

We conclude that building on the analogy between a laser-induced *e-h* plasma in condensed matter systems and the plasma created in the collision of elementary particles, or with primordial conditions in the Universe, gives us a practical laboratory-scale playground for the exploration of temporally evolving systems though symmetry breaking transitions. Remarkably, the CDW model system give rise to two kinds of cosmological analogies, namely of the AM as the analogue to the Higgs boson and odd-symmetry phonons as dark matter excitations. The CDW systems reveal some hitherto unexplored bosonic excitations created under nonequilibrium conditions which may be expected to have observable counterparts in other temporally evolving systems. The reflectivity response function derived for a superconductor allows the investigation of the trajectory of the order parameter through the transition, opening the way to studies of intrinsic vortex dynamics.

7. Acknowledgments

We wish to acknowledge discussions with Prof. T. Kibble on the importance of varying the quench rate in these experiments. We also acknowledge the use of $DyTe_3$ and LaSrCuO single crystal samples kindly provided by I. Fischer and S. Sugai respectively.

References

[1] Kabanov V, Demsar J, Podobnik B and Mihailovic D 1999 Quasiparticle relaxation dynamics in superconductors with different gap structures: Theory and experiments on $YBa_2Cu_3O_{7-\delta}$ Phys Rev B 59 1497–506

[2] Gadermaier C, Kabanov V V, and Alexandrov A S et al 2012 arXiv 1205.4978, ibid 2010 Phys Rev Lett 105 257001.

[3] Schmid A and Schön G 1975 Linearized kinetic equations and relaxation processes of a superconductor near Tc J Low Temp Phys 20 207–27, Gor'kov L P and Kopnin N B 1975 *Soviet Physics Uspekhi* 18 496

[4] Demsar J, Biljakovic K and Mihailovic D 1999 Single particle and collective excitations in the one-dimensional charge density wave solid $K_{0.3}MoO_3$ probed in real time by femtosecond spectroscopy Phys Rev Lett 83 800–3

[5] Yusupov R V, Mertelj T, Chu J H, Fisher I R and Mihailovic D 2008 Single-Particle and Collective Mode Couplings Associated with 1-and 2-Directional Electronic Ordering in Metallic RTe_3 (R=Ho,Dy,Tb) Phys Rev Lett 101 246402

[6] Zurek W 1985 Cosmological experiments in superfluid helium? Nature 317 505

[7] Kibble T 1976 Topology of cosmic domains and strings. J Phys A-Math Gen 9 1387–98
[8] Monaco R, Mygind J, Aaroe M, Rivers R J and Koshelets V P 2006 Zurek-Kibble Mechanism for the Spontaneous Vortex Formation in Nb-Al/Al_{ox}/Nb Josephson Tunnel Junctions: New Theory and Experiment Phys Rev Lett 96 180604
[9] Golubchik D, Polturak E and Koren G 2010 Evidence for Long-Range Correlations within Arrays of Spontaneously Created Magnetic Vortices in a Nb Thin-Film Superconductor Phys Rev Lett 104 247002
[10] Weiler C N, Neely T W, Scherer D R, Bradley A S, Davis M J and Anderson B P 2008 Spontaneous vortices in the formation of Bose–Einstein condensates Nature 455 948–51
[11] Roumpos G, Fraser M, Löffler A and Höfling S 2011 Single vortex-antivortex pair in an exciton-polariton condensate Nat Phys 7 129
[12] Yusupov R, Mertelj T, Kabanov V V, Brazovskii S, Kusar P, Chu J-H, Fisher I R and Mihailović D 2010 Coherent dynamics of macroscopic electronic order through a symmetry breaking transition Nat Phys 6 681–4
[13] Yusupov R, Mertelj T, Kabanov V V, Kusar P, Mihailovic D, Chu J-H, Fisher I R and Brazovskii S 2010 Femtosecond Coherent Non-equilibrium Electronic Ordering and Dynamics of Topological Defect in Charge Density Waves J Supercond Nov Magn 24 1191
[14] Ivlev B I, Kopnin N B 1984 Electronic currents and resistive states in thin superconductors Adv Phys 33 47
[15] Lu-Dac M and Kabanov V 2009 Multiple phase slips phenomena in mesoscopic superconducting rings, 2009 Phys Rev B 79 184521
[16] Allen P 1987 Theory of thermal relaxation of electrons in metals Phys Rev Lett 59 1460–3
[17] Ginzburg V L 1963 Sov. Phys. Usp. 5, 649 (1963), Ginzburg V L, Levanyuk A P, Sobianin A A 1980 Uspekhi Fizicheskih Nauk 130 615
[18] Kabanov V V and Alexandrov A S 2008 Electron relaxation in metals: Theory and exact analytical solutions Phys Rev B 78 174514
[19] Hai-Hu Wen et al. 2004 Phys Rev B70 214505
[20] Kusar P, Kabanov V, Demsar J and Mertelj T 2008 Controlled Vaporization of the Superconducting Condensate in Cuprate Superconductors by Femtosecond Photoexcitation Phys Rev Lett 101 227001. (Note that in this paper the formula for R (eq. 1) erroneously gives Δ instead of Δ^2 , which is corrected in subsequent works.)
[21] Kabanov V.V., Demsar J, Podobnik B, and Mihailovic D, 1999, Phys Rev B 59, 1497.
[22] Kabanov V, Demsar J and Mihailovic D 2005 Kinetics of a superconductor excited with a femtosecond optical pulse Phys Rev Lett 95 147002
[23] Rothwarf A and Taylor B 1967 Measurement of recombination lifetimes in superconductors Phys Rev Lett 19 27
[24] Ru N et al. Effect of chemical pressure on the charge density wave transition in rare earth tritellurides RTe_3 2008 Phys Rev B 77 035114
[25] Degiorgi L (2010) unpublished optical constant data.
[26] Mertelj T, Kabanov V V, Fisher I and Mihailovic D 2013 Incoherent topological defecgt recombination dynamics in $TbTe_3$. Phys Rev Lett 110 156401